

# Metal Ion Induced Self-Assembly of a Designed Peptide into a Triple-Stranded $\alpha$ -Helical Bundle: A Novel Metal Binding Site in the Hydrophobic Core

Kazuo Suzuki, Hidekazu Hiroaki, Daisuke Kohda, Haruki Nakamura, and Toshiki Tanaka\*

Contribution from the Biomolecular Engineering Research Institute, 6-2-3, Furuedai, Suita, Osaka 565-0874, Japan

Received August 3, 1998

**Abstract:** Coiled coils, which mediate the associations and regulate the functions of various proteins, have a representative amino acid sequence of (defgabc)<sub>n</sub> heptad repeats and usually have hydrophobic residues at the a and d positions. We have designed a triple-stranded parallel  $\alpha$ -helical coiled coil, in which the amino acid sequence is YGG(IKKIEA)<sub>4</sub>. To construct a peptide that undergoes metal ion induced self-assembly into a triple-stranded coiled coil, we engineered a metal binding site in the hydrophobic core of the coiled coil. We replaced two Ile residues of the third heptad with His residues. The peptide had a random structure in aqueous solution. In contrast, in the presence of a transition metal ion, the peptide exhibited an  $\alpha$ -helical conformation. The metal-complexed peptide was triple stranded and had a parallel orientation, as determined by sedimentation equilibrium and fluorescence quenching analyses. Metal ion titrations monitored by circular dichroism revealed that the dissociation constants,  $K_d$ , were  $35 \pm 1 \mu\text{M}$  for Co(II),  $5.0 \pm 0.3 \mu\text{M}$  for Ni(II),  $17 \pm 1 \mu\text{M}$  for Cu(II), and  $23 \pm 2 \mu\text{M}$  for Zn(II). The Ni(II) binds to the His residues, as judged by both pH titration monitored by circular dichroism and metal ion titration monitored by nuclear magnetic resonance. The highest affinity for Ni(II) suggests that the metal binding site has six-coordinated octahedral geometry. Thus, the peptide is a useful tool to control the associations of functional domains attached to the peptide.

## Introduction

The ultimate goals of the de novo design of proteins are the understanding of natural proteins and the creation of novel functional proteins. In recent studies, several secondary and tertiary structures have been de novo designed and constructed by peptide chemistry. The target structures include various motifs, such as  $\alpha$ -helical bundles,<sup>1</sup> coiled coils,<sup>2</sup> collagens,<sup>3</sup>  $\beta$ -sheet proteins,<sup>4</sup>  $\alpha/\beta$  proteins,<sup>5</sup> and Zn-finger motifs.<sup>6</sup> In

particular,  $\alpha$ -helical bundles and coiled coils have been the subjects of extensive protein design because of their structural simplicity and functional diversity. Although previously designed helical proteins had a tendency to form molten globules,<sup>7</sup> significant progress has recently been made in the design of native-like helical proteins.<sup>8</sup>

Coiled coils, which contain a heptad sequence repeat, mediate the associations of numerous natural proteins.<sup>9</sup> In addition, both natural and designed coiled coils were also fused to various functional domains of natural proteins to assist their self-assembly.<sup>10</sup> Furthermore, there are several coiled coil domains, which not only mediate the associations but also regulate the functions of natural proteins via large conformational rearrange-

\* To whom correspondence should be addressed. Telephone: +81-6-872-8208. Fax: +81-6-872-8219. E-mail: ttanaka@beri.co.jp.

(1) (a) Ho, S. P.; DeGrado, W. F. *J. Am. Chem. Soc.* **1987**, *109*, 6751–6758. (b) Hecht, M. H.; Richardson, J. S.; Richardson, D. C.; Ogden, R. C. *Science* **1990**, *249*, 884–891. (c) Handel, T. M.; Williams, S. A.; DeGrado, W. F. *Science* **1993**, *261*, 879–885.

(2) Lau, S. Y. M.; Taneja, A. K.; Hodges, R. S. *J. Biol. Chem.* **1984**, *259*, 13253–13261. (b) O'Neil, K. T.; DeGrado, W. F. *Science* **1990**, *250*, 646–651. (c) Harbury, P. B.; Zhang, T.; Kim, P. S.; Alber, T. *Science* **1993**, *262*, 1401–1407.

(3) Fields, G. B.; Prockop, D. J. *Biopolymers* **1996**, *40*, 345–357.

(4) (a) Moser, R. M.; Thomas, B.; Gutte, B. *FEBS Lett.* **1983**, *157*, 247–251. (b) Pessi, A.; Bianchi, E.; Cramer, A.; Venturini, S.; Tramontano, A.; Sollazzo, M. *Nature* **1993**, *362*, 367–369. (c) Quin, T. P.; Tweedy, N. B.; Williams, R. W.; Richardson, J. S.; Richardson, D. C. *Proc. Natl. Acad. Sci. U.S.A.* **1994**, *91*, 8747–8751.

(5) (a) Beuregard, M.; Goraj, K.; Goffin, V.; Heremans, K.; Goormaghtigh, E.; Ruyschaert, J.; Martial, J. A. *Protein Eng.* **1991**, *4*, 745–749. (b) Fedorov, A. N.; Dolgikh, D. A.; Chemeris, V. V.; Chernov, B. K.; Finkelstein, A. V.; Schulga, A. A.; Alakhov, Y. B.; Kirpichnikov, M. P.; Pitsyn, O. B. *J. Mol. Biol.* **1992**, *225*, 927–931. (c) Tanaka, T.; Kimura, H.; Hayashi, M.; Fujiyoshi, Y.; Fukuhara, K.; Nakamura, H. *Protein Sci.* **1994**, *3*, 419–427.

(6) (a) Krizek, B. A.; Amann, B. T.; Kilfoil, V. J.; Merkle, D. L.; Berg, J. M. *J. Am. Chem. Soc.* **1991**, *113*, 4518–4523. (b) Michael, S. F.; Kilfoil, V. J.; Schmidt, M. H.; Amann, B. A.; Berg, J. M. *Proc. Natl. Acad. Sci. U.S.A.* **1992**, *89*, 4796–4800.

(7) Betz, S. F.; Raleigh, D. P.; DeGrado, W. F. *Curr. Opin. Struct. Biol.* **1993**, *3*, 601–610.

(8) (a) Raleigh, D. P.; Betz, S. F.; DeGrado, W. F. *J. Am. Chem. Soc.* **1995**, *117*, 7558–7559. (b) Lumb, K. J.; Kim, P. S. *Biochemistry* **1995**, *34*, 8642–8648. (c) Betz, S. F.; Bryson, J. W.; DeGrado, W. F. *Curr. Opin. Struct. Biol.* **1995**, *5*, 457–463. (d) Betz, S. F.; Liebman, P. A.; DeGrado, W. F. *Biochemistry* **1997**, *36*, 2450–2458. (e) Johansson, J. S.; Gibney, B. R.; Skalicky, J. J.; Wand, A. J.; Dutton, P. L. *J. Am. Chem. Soc.* **1998**, *120*, 3881–3886. (f) Suzuki, K.; Hiroaki, H.; Kohda, D.; Tanaka, T. *Protein Eng.*, in press.

(9) (a) Cohen, C.; Parry, D. A. D. *Proteins* **1990**, *7*, 1–15. (b) Lupas, A. *Trends Biochem. Sci.* **1996**, *21*, 375–382.

(10) (a) Hu, J. C.; O'Shea, E. K.; Kim, P. S.; Sauer, R. T. *Science* **1990**, *250*, 1400–1403. (b) Schmidt-Dörr, T.; Oertel-Buchheit, P.; Pernelle, C.; Bracco, L.; Schnarr, M.; Granger-Schnarr, M. *Biochemistry* **1991**, *30*, 9657–9664. (c) Blondel, A.; Bedouelle, H. *Protein Eng.* **1991**, *4*, 457–461. (d) Wu, A.; Eaton, S. F.; Laue, T. M.; Johnson, K. W.; Sana, T. R.; Ciardelli, T. L. *Protein Eng.* **1994**, *7*, 1137–1144. (e) Pack, P.; Müller, K.; Zahn, R.; Plückthun, A. *J. Mol. Biol.* **1995**, *246*, 28–34. (f) Kruijff, J.; Logtenberg, T. *J. Biol. Chem.* **1996**, *271*, 7630–7634. (g) Weissenhorn, W.; Dessen, A.; Harrison, S. C.; Skehel, J. J.; Wiley, D. C. *Nature* **1997**, *387*, 426–430.

ments in response to environmental changes. For example, the coiled coil domains in influenza hemagglutinin and the macrophage scavenger receptor exhibit pH-dependent conformational changes, causing membrane fusion of the virus and ligand release from the receptor, respectively.<sup>11,12</sup> The heat shock transcription factor regulates the expression of the heat shock elements, via a conformational change of the coiled coil domain in response to temperature.<sup>13</sup> Therefore, designed coiled coil peptides, which drastically change their conformation depending on external stimuli, are useful tools to control the associations and the functions of domains attached to peptides.

Among the various external stimuli, metal binding is one of the most attractive targets, since metal ions play important roles in many biological systems and the factors required for metal binding are well understood. Actually, the engineering of metal binding sites in proteins and peptides is receiving an increasing amount of attention.<sup>14</sup> Most of the metal binding sites are, however, designed into preformed structures. Synthetic peptides derived from the muscle protein troponin-C were demonstrated to undergo  $\text{Ca}^{2+}$ -induced folding and dimerization.<sup>15</sup> A very successful design to induce a drastic conformational change was recently reported by Hodges and co-workers.<sup>16</sup> They designed a disulfide-linked double-stranded coiled coil, designated as  $\text{Gla}_2\text{Nx}$ , which underwent a random coil to coiled coil transition upon lanthanide ion binding to the solvent-exposed  $\gamma$ -carboxyglutamic acid.

Recent effort have focused on the design of triple-stranded coiled coils, rather than double-stranded coiled coils.<sup>17</sup> Several homo- and heterotrimeric coiled coils were also successfully designed.<sup>2c,18</sup> We previously constructed a nativelike triple-stranded coiled coil peptide (IZ), in which the amino acid sequence is YGG(IEKKIEA)<sub>4</sub>.<sup>8f</sup> In this paper, we designed a peptide that undergoes metal ion induced self-assembly into a triple-stranded coiled coil. For this purpose, two His residues were substituted for two Ile residues in the third heptad of the IZ. The hydrophilic His residues in the hydrophobic core would greatly destabilize the coiled coil structure and favor a random coil structure. In the presence of a transition metal ion, however, metal ion binding to de novo octahedral six-coordinate sites in the hydrophobic core would facilitate the formation of a triple-stranded coiled coil. The design, structural properties, metal binding behavior, and postulated coordination geometry of the metalloprotein IZ-3adH are reported herein.

## Experimental Section

**Peptide Synthesis.** The peptide, IZ-3adH, was synthesized by the solid-phase peptide synthesis method using Rink amide resin,<sup>19</sup>  $\text{N}^\alpha$ -Fmoc-protected amino acids, HBTU, and hydroxybenzotriazole on an Applied Biosystems peptide synthesizer, model 430A. Deprotection and cleavage were performed by treatment with TFA containing 5% ethanedithiol and anisole (1/3, v/v) for 1.5 h. Peptide purification was carried out at room temperature by reversed-phase HPLC using a YMC-pack ODS-A column (10 mm i.d.  $\times$  250 mm, 120 Å, 5  $\mu\text{m}$ , YMC Inc., Japan) eluted at 3 mL/min. A linear elution gradient was used with 25–40%  $\text{CH}_3\text{CN}/\text{H}_2\text{O}$  containing 0.1% TFA during 30 min. The final product was characterized by analytical HPLC and MALDI-TOF mass spectrometry.

For the fluorescence quenching assay, a Cys residue was coupled to the N-terminus of the IZ-3adH peptide. After deprotection and purification as above, the peptide was dissolved in 500  $\mu\text{L}$  of 0.2 M acetate buffer (pH 4.0) to a peptide concentration of about 300  $\mu\text{M}$ . *N*-(9-Acridinyl) maleimide (DOJINDO, Japan) was dissolved in 350  $\mu\text{L}$  of acetone (3 mM) and then was mixed with the peptide solution. After 1 h at room temperature, the acridinyl IZ-3adH was purified by reversed phase HPLC.

**Modeling Procedure.** The entire backbone structure of IZ-3adH was first built on the basis of the X-ray crystal structure of the GCN4 Leu zipper core mutant, P-II (PDB code, 1GCM).<sup>20</sup> The octahedral His- $\text{X}_3$ -His site with Ni(II) was constructed by imposing distance restraints between each  $\text{N}\epsilon_2$  atom and Ni(II), which were assumed to be 2.13 Å from the distance between N and Ni(II) in the crystal structure of tris-(ethylenediamine)nickel(II).<sup>21</sup> All of the other optimum side-chain conformers, except for the His residues, were selected using the dead-end elimination algorithm.<sup>22</sup> Using the molecular mechanics program, PRESTO,<sup>23</sup> with an AMBER all atom force field,<sup>24</sup> the structure was optimized and the bad contacts were minimized by the conjugate gradient method.

**Circular Dichroism (CD).** All CD measurements were carried out on a JASCO 720 spectrometer at a peptide concentration of 20  $\mu\text{M}$ . The mean residue ellipticity,  $[\theta]$ , is given in units of  $\text{deg cm}^2 \text{dmol}^{-1}$ . The peptide concentration was determined by measuring the tyrosine absorbance in 6 M guanidine hydrochloride solutions, using  $\epsilon_{275} = 1450 \text{ M}^{-1} \text{ cm}^{-1}$ .<sup>25</sup> For the preparation of a metal stock solution, the metal chloride was dissolved in buffer that had been purged with nitrogen for deoxygenation.

CD spectra were measured in 10 mM sodium phosphate and 100 mM NaCl (pH 7.0) in the presence and absence of Co(II), Ni(II), Cu(II), or Zn(II) (20  $\mu\text{M}$ ). The thermal transition analysis was performed in 10 mM Tris-HCl, 100 mM NaCl, and 30  $\mu\text{M}$   $\text{NiCl}_2$  at pH 7.4. The  $[\theta]$  at 222 nm ( $[\theta]_{222}$ ) was monitored as a function of temperature. The temperature was increased at a rate of 1  $^\circ\text{C}/\text{min}$ . The thermal transition was reversible. To determine the effect of pH on the  $\alpha$ -helical content, the  $[\theta]_{222}$  was monitored as a function of pH from 4.3 to 7.4 in the same buffer at 20  $^\circ\text{C}$ .

Metal ion titrations were also performed in 10 mM Tris-HCl and 100 mM NaCl (pH 7.4) at 20  $^\circ\text{C}$ , by monitoring the  $[\theta]_{222}$  as a function

(11) Carr, C. M.; Kim, P. S. *Cell* **1993**, *73*, 823–832.

(12) (a) Doi, T.; Kurasawa, M.; Higashino, K.; Imanishi, T.; Mori, T.; Naito, M.; Takahashi, K.; Kawabe, Y.; Wada, Y.; Matsumoto, A.; Kodama, T. *J. Biol. Chem.* **1994**, *269*, 25598–25604. (b) Suzuki, K.; Doi, T.; Imanishi, T.; Kodama, T.; Tanaka, T. *Biochemistry* **1997**, *36*, 15140–15146.

(13) (a) Rabindran, S. K.; Haroun, R. I.; Clos, J.; Wisniewski, J.; Wu, C. *Science* **1993**, *259*, 230–234. (b) Sorger, P. K.; Nelson, H. C. M. *Cell* **1989**, *59*, 807–813.

(14) (a) Regan, L. *Trends Biochem. Sci.* **1995**, *20*, 280–285. (b) Lu, Y.; Valentine, J. S. *Curr. Opin. Struct. Biol.* **1997**, *7*, 495–500. (c) Hellinga, H. W. *Fold. Des.* **1998**, *3*, R1–R8.

(15) Shaw, G. S.; Findlay, W. A.; Semchuk, P. D.; Hodges, R. S.; Sykes, B. D. *J. Am. Chem. Soc.* **1992**, *114*, 6248–6259.

(16) Kohn, W. D.; Kay, C. M.; Sykes, B. D.; Hodges, R. S. *J. Am. Chem. Soc.* **1998**, *120*, 1124–1132.

(17) Schneider, J. P.; Lombardi, A.; DeGrado, W. F. *Fold. Des.* **1998**, *3*, R29–R40.

(18) (a) Nautiyal, S.; Woolfson, D. N.; King, D. S.; Alber, T. *Biochemistry* **1995**, *34*, 11645–11651. (b) Boice, J. A.; Dieckmann, G. R.; DeGrado, W. F.; Fairman, R. *Biochemistry* **1996**, *35*, 14480–14485. (c) Lombardi, A.; Bryson, J. W.; DeGrado, W. F. *Biopolymers* **1996**, *40*, 495–504.

(19) Abbreviations: Rink amide resin, 4-(2',4'-dimethoxyphenyl)-Fmoc-aminomethylphenoxy resin; Fmoc, 9-fluorenylmethoxycarbonyl; HBTU, 2-(1*H*-benzotriazole-1-yl)-1,1,3,3-tetramethyluronium hexafluorophosphate; TFA, trifluoroacetic acid; HPLC, high-performance liquid chromatography; MALDI-TOF, matrix-assisted laser desorption/ionization time-of-flight; CD, circular dichroism; Tris-HCl, tris(hydroxymethyl)aminomethane hydrochloride;  $K_d$ , dissociation constant;  $\Delta G_{\text{diss}}$ , dissociation free energy;  $k_{\text{ex}}$ , observed amide exchange rate constant;  $k_{\text{int}}$ , average intrinsic amide exchange rate constant;  $K_{\text{op}}$ , unfolding equilibrium constant;  $\Delta G_{\text{op}}$ , unfolding free energy.

(20) Harbury, P. B.; Kim, P. S.; Alber, T. *Nature* **1994**, *371*, 80–83.

(21) Cramer, R. E.; van Doorne, W.; Huneke, J. T. *Inorg. Chem.* **1976**, *15*, 529–535.

(22) (a) Desmet, J.; De Maeyer, M.; Hazes, B.; Lasters, I. *Nature* **1992**, *356*, 539–542. (b) Tanimura, R.; Kidera, A.; Nakamura, H. *Protein Sci.* **1994**, *3*, 2358–2365.

(23) Morikami, K.; Nakai, T.; Kidera, A.; Saito, M.; Nakamura, H. *Comput. Chem.* **1992**, *16*, 243–248.

(24) Weiner, S. J.; Kollman, P. A.; Nguyen, D. T.; Case, D. J. *Comput. Chem.* **1986**, *7*, 230–252.

(25) Brandts, J. R.; Kaplan, K. J. *Biochemistry* **1973**, *12*, 2011–2024.

of the metal concentrations, which were varied between 0.1 and 25.6  $\mu\text{M}$  for Ni(II) and between 1  $\mu\text{M}$  and 1 mM for the other metal ion, respectively. The molar fraction of folded peptide ( $f$ ) was calculated from the equation  $f = ([\theta] - [\theta]_f)/([\theta]_s - [\theta]_f)$ , where  $[\theta]$  is the observed  $[\theta]_{222}$  at a particular point in the titration and  $[\theta]_f$  and  $[\theta]_s$  are the  $[\theta]_{222}$  values of the metal-free and metal-saturated forms of the peptide, respectively. In this study, the  $[\theta]_{222}$  values measured at the peptide and the metal concentrations of 100 and 200  $\mu\text{M}$ , respectively, were used as the  $[\theta]_s$ .

As discussed below, a single metal ion is bound to three peptide molecules. Metal ion titration data were analyzed for a two-state model,  $1/3\text{M} + \text{P} \leftrightarrow 1/3(\text{P}_3\text{M})$ . The dissociation constant  $K_d$  is defined as

$$K_d = [\text{P}][\text{M}]^{1/3}/[\text{P}_3\text{M}]^{1/3} \quad (1)$$

where  $[\text{P}]$  is the free peptide concentration,  $[\text{M}]$  is the free metal concentration, and  $[\text{P}_3\text{M}]$  is the peptide-metal complex concentration. Equation 1 is expressed in terms of the total peptide concentration,  $P_t$ , and the total metal concentration,  $M_t$

$$K_d = (P_t - fP_t)(M_t - fP_t/3)^{1/3}/(fP_t/3)^{1/3} \quad (2)$$

Rearranging the terms of eq 2 yields

$$M_t = f\{[K_d^3/3P_t^2(1 - f)^3] + P_t/3\} \quad (3)$$

The  $K_d$  and the associated error for the metal were determined from a nonlinear least-squares fit of eq 3, using the KaleidaGraph program (Synergy Software). The dissociation free energy per peptide chain,  $\Delta G_{\text{diss}}$ , is calculated from eq 4

$$\Delta G_{\text{diss}} = -RT \ln K_d \quad (4)$$

where  $R$  is the gas constant and  $T$  is the absolute temperature.

**Sedimentation Equilibrium Ultracentrifugation.** Sedimentation equilibrium analysis was performed with a Beckman XL-1 Optima Analytical Ultracentrifuge equipped with absorbance optics. The initial peptide concentration was 100  $\mu\text{M}$  in 10 mM sodium phosphate and 100 mM NaCl (pH 7.4) containing NiCl<sub>2</sub> (500  $\mu\text{M}$ ) or in 10 mM Tris-HCl and 100 mM NaCl (pH 7.5) containing CoCl<sub>2</sub>, CuCl<sub>2</sub>, or ZnCl<sub>2</sub> (200  $\mu\text{M}$ ). The sample was centrifuged at 25 000 rpm at 25 °C, and the absorbance was monitored at 280 nm. The oligomerization state was determined by fitting the data to a single species without considering any influences of the metals, using Origin Sedimentation Equilibrium Single Data Set Analysis (Beckman). The partial specific volume used for the data analysis was 0.758 mL/g, calculated from the weighted average of the amino acid content using the method of Cohn and Edsall.<sup>26</sup>

**Fluorescence Quenching Assay.** The fluorescence quenching assay was performed with a HITACHI F-4500 fluorescence spectrophotometer with a 1-cm path-length cuvette. The emission spectra between 390 and 550 nm of the acridinyl peptides were measured with excitation at 362 nm. The measurements were performed in 10 mM Tris-HCl and 100 mM NaCl (pH 7) containing the indicated concentrations of NiCl<sub>2</sub> at room temperature. The concentration of each peptide was about 20  $\mu\text{M}$ .

**Nuclear Magnetic Resonance (NMR).** NMR spectroscopy was performed on a Bruker DMX600 spectrometer operated at 600.13 MHz for <sup>1</sup>H. Chemical shifts were referenced internally to 0 ppm with trimethylsilylpropionic acid. One-dimensional spectra were measured at 25 °C with suppression of the residual water signal by weak presaturation. The data sets were defined by 8 k complex points, and 32 scans were accumulated using a spectral width of 8289.3 Hz. Samples were prepared at an approximate concentration of 1 mM in <sup>2</sup>H<sub>2</sub>O (pH 7.0). In the Ni(II) titration study, small aliquots of a NiCl<sub>2</sub> solution were added to the peptide solution, with a total volume change of about 10% over the titration.

(26) Cohn, E. J.; Edsall, J. T. *Proteins, Amino Acids and Peptides as Ions and Dipolar Ions*; Reinhold Publishing Corp.: New York, 1943; pp 370–381.

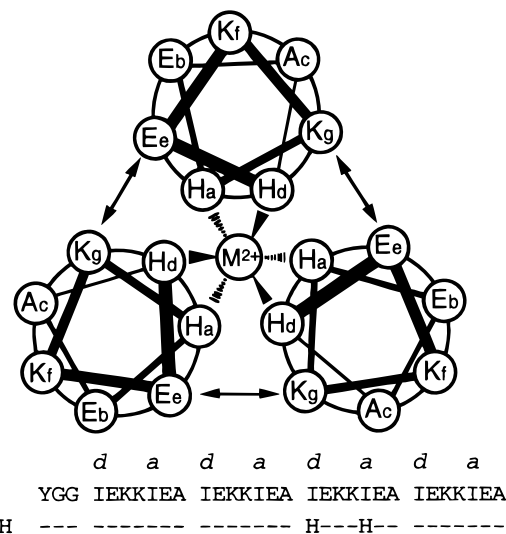


**Figure 1.** Helical wheel representation of the third heptad of the IZ-3adH in the parallel orientation, viewed from the N- to the C-terminus. Sequences of the IZ and the IZ-3adH are also represented. The four heptad repeats are preceded by the YGG sequence for the peptide quantitation. The Glu and Lys residues at the e and g positions undergo electrostatic interactions between adjacent helices. The side chains of the His residues in the IZ-3adH form a metal binding site with octahedral six-coordinate geometry.

The hydrogen exchange study was initiated by dissolving the lyophilized peptide and the NiCl<sub>2</sub> in <sup>2</sup>H<sub>2</sub>O. The concentrations of the peptide and the NiCl<sub>2</sub> were 1 and 0.4 mM, respectively. An observed exchange rate constant ( $k_{\text{ex}}$ ) was calculated from a two-parameter nonlinear least-squares fit of the exponential decay curve of the peak intensities between 5 min and 5 h, using KaleidaGraph. The average intrinsic amide exchange rate ( $k_{\text{int}}$ ) was 31 s<sup>-1</sup>, corresponding to three times the rate of amide exchange for poly-DL-alanine at pH 7 and 25 °C.<sup>8b,27</sup> Natural globular proteins typically contain a subset of amide protons that undergo hydrogen exchange only from the globally unfolded protein. This feature is a hallmark of nativelike levels of structural uniqueness.<sup>28</sup> When exchange occurs from the globally unfolded protein, and the folded protein is stable ( $f_u \ll 1$ ),  $K_{\text{op}}$  is, in principle, equal to  $k_{\text{ex}}/k_{\text{int}}$ , where  $K_{\text{op}}$  is the unfolding equilibrium constant of a single IZ-3adH in the peptide-metal complex.<sup>29</sup> The unfolding free energy,  $\Delta G_{\text{op}}$ , is expressed as  $-RT \ln K_{\text{op}}$ .

## Results

**Metallopeptide Design.** Previous efforts on metallopeptide design provided clues for designing the metal ion induced self-assembly of a peptide. The formation of a monomeric  $\alpha$ -helix was promoted by a single transition metal ion binding to a His-X<sub>3</sub>-His site in a peptide sequence with an octahedral two-coordinate geometry.<sup>30</sup> There were still four nonligated metal coordination sites remaining. They could be occupied by two additional His-X<sub>3</sub>-His sites, which might facilitate the association of the three peptide molecules into a triple-stranded  $\alpha$ -helical bundle. In this case, the metal binding site would exist in the interior of the  $\alpha$ -helical bundle. Therefore, to construct a self-assembling peptide, we designed a metal binding site in the hydrophobic interior of the parallel triple-stranded coiled coil peptide.

(27) Englander, S. W.; Downer, N. W.; Teitelbaum, H. *Annu. Rev. Biochem.* **1972**, *41*, 903–924.

(28) (a) Roder, H. *Methods Enzymol.* **1989**, *176*, 446–473. (b) Bai, Y., Milne, J. S.; Mayne, L.; Englander, S. W. *Proteins* **1994**, *20*, 4–14.

(29) Dürr, E.; Bosshard, H. R. *Eur. J. Biochem.* **1997**, *249*, 325–329.

(30) (a) Ghadiri, M. R.; Choi, C. *J. Am. Chem. Soc.* **1990**, *112*, 1630–1632. (b) Arnold, F. H.; Haymore, B. *Science* **1991**, *252*, 1796–1797.



**Figure 2.** Tertiary model of the Ni(II) complex of the IZ-3adH. A side view (right) and a bottom view from the C-termini (left) of the peptide-metal complex are shown. The six His side chains are shown by the sticks with the three helix backbones. The Ni(II) is indicated by a sphere.

We previously prepared a parallel triple-stranded coiled coil, IZ, which showed extremely high thermal stability and nativelike properties.<sup>8f</sup> The IZ peptide consists of 31 amino acid residues with four repeats of the heptad, I<sub>d</sub>E<sub>c</sub>K<sub>f</sub>K<sub>g</sub>I<sub>a</sub>E<sub>b</sub>A<sub>c</sub> (Figure 1). To create the metal binding His-X<sub>3</sub>-His site inside the  $\alpha$ -helical coiled coil structure, we substituted two His residues for the Ile residues at the d and a positions of the third heptad of the IZ, designated as IZ-3adH. In the parallel coiled coil structure, these His residues could be positioned near the six corners of an octahedron. We made a computer model, in which the single Ni(II) ion is bound inside the triple-stranded IZ-3adH (Figure 2). The model thus obtained shows that the  $\epsilon$ -N atoms of the six His residues provide a metal binding site with good octahedral geometry. In the model, the peptide-metal complex forms  $\Lambda$  facial isomers, in which one face is formed by three His residues at the d layer and the other face by three His residues at the a layer (Figures 1 and 2).

To undergo metal ion induced self-assembly, a designed peptide should be completely unfolded in the absence of the metal ion. The two His residues of the IZ-3adH would exist in the hydrophobic core of the coiled coil structure. Since the hydrophilic His residues in the hydrophobic core would greatly destabilize the coiled coil structure,<sup>1c</sup> the IZ-3adH is expected to form a random coil structure in the absence of a transition metal ion.

**Structural Characterization of IZ-3adH.** The CD spectra of the IZ-3adH were measured in a benign buffer at pH 7 and

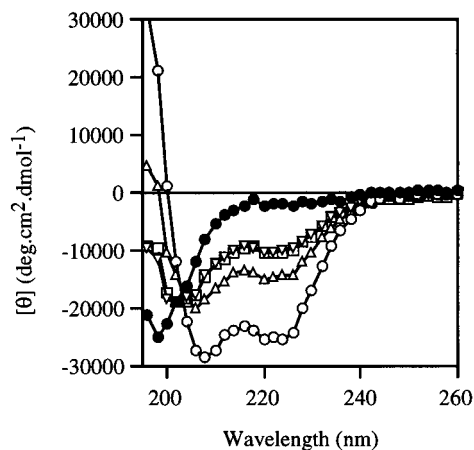


**Figure 3.** Circular dichroism spectra of the IZ-3adH peptide in the absence (closed circles) and presence (open symbols) of the metal ion (CoCl<sub>2</sub>, squares; NiCl<sub>2</sub>, circles; CuCl<sub>2</sub>, triangles; ZnCl<sub>2</sub>, inverted triangles). The measurements were performed in 10 mM sodium phosphate containing 0.1 M NaCl (pH 7.0) at 20 °C. The peptide concentrations were 20  $\mu$ M.

are shown in Figure 3. In contrast to the IZ, which formed a stable coiled coil structure under these conditions,<sup>8f</sup> the CD spectrum of the IZ-3adH in the absence of transition metal ions is characteristic of a random coil structure, with a minimum at 196 nm. A significant change of the CD spectra was not

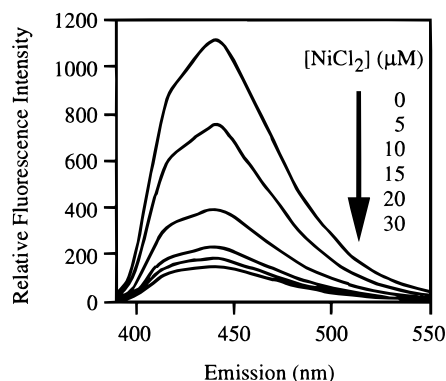


**Figure 4.** Fluorescence spectra of the acridinyl IZ-3adH in the presence of  $\text{NiCl}_2$ . The spectra of the acridinyl peptide were obtained with excitation at 362 nm, at a peptide concentration of about 20  $\mu\text{M}$ . Measurements were performed at room temperature in 10 mM Tris-HCl and 100 mM NaCl (pH 7.0) containing the indicated concentrations of  $\text{NiCl}_2$ .

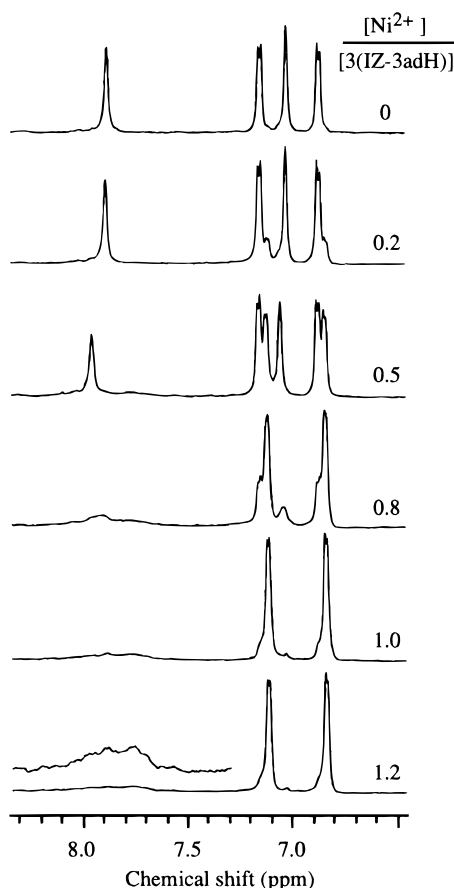


**Figure 5.** One-dimensional  $^1\text{H}$  NMR spectra of the IZ-3adH. Measurements were performed in  $^2\text{H}_2\text{O}$  (pH 7) at the peptide concentration of 1 mM, corresponding to 0.33 mM of the trimerized IZ-3adH. The concentrations of  $\text{NiCl}_2$  were 0, 0.07, 0.17, 0.27, 0.33, and 0.40 mM, respectively. The spectrum in the absence of  $\text{Ni}(\text{II})$  was assigned: 6.87 ppm (Tyr,  $\delta$ -CH), 7.03 (His,  $\delta$ -CH), 7.20 (Tyr,  $\epsilon$ -CH), 7.90 (His,  $\epsilon$ -CH).

observed at the peptide concentration between 20 and 400  $\mu\text{M}$ . This result indicates that the substitutions of His for Ile at the d and a positions almost completely destabilize the coiled coil structure, as we expected. To analyze the metal ion induced folding of the IZ-3adH, we used transition metals, including Co(II), Ni(II), Cu(II), and Zn(II). As shown in Figure 3, the spectra of the IZ-3adH became typical of an  $\alpha$ -helical structure, with minima at 208 and 222 nm, upon the addition of any metal

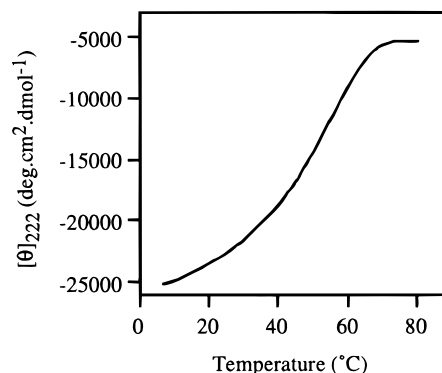


**Figure 6.** Thermal melting curves of the IZ-3adH in the presence of  $\text{NiCl}_2$ . The mean residue ellipticity at 222 nm of the peptide was monitored as a function of temperature. The thermal transition was performed in 10 mM Tris-HCl, 100 mM NaCl (pH 7.4), and 30  $\mu\text{M}$   $\text{NiCl}_2$ . The peptide concentration was 20  $\mu\text{M}$ .

ion. In particular, remarkable  $\alpha$ -helical formation was observed in the presence of  $\text{Ni}(\text{II})$ . The ratio of  $[\theta]_{222}$  and  $[\theta]_{208}$  ( $[\theta]_{222}/[\theta]_{208}$ ) for a coiled coil structure is usually greater than 1,<sup>31</sup> while the  $\text{Ni}(\text{II})$ -complexed IZ-3adH showed a  $[\theta]_{222}/[\theta]_{208}$  of about 0.88. This result suggests that the metal-complexed peptide forms either a partially unfolded coiled coil or, more likely, an  $\alpha$ -helical bundle.

The oligomerization states of the metal-complexed IZ-3adH were determined by sedimentation equilibrium centrifugation analyses.<sup>32</sup> Each sample was centrifuged at the peptide and the metal ion concentrations of 100 and 200–500  $\mu\text{M}$ , respectively. The data for the peptide–metal complex, except Cu(II), were fitted to a single species. The residuals are random and centered around zero, indicating that the peptide–metal complex sediments as a single homogeneous species. The apparent molecular size of the metal-complexed peptide was 10 613 for Co(II), 10 112 for Ni(II), and 10 613 Da for Zn(II). These results indicate that the metal-complexed IZ-3adH was trimerized (the calculated molecular mass for the trimerized peptide is 10 771 Da). The data for Cu(II)-complexed peptide could not be fitted, presumably due to the influence of the absorption of Cu(II).

There are two possible helical orientations of a triple-stranded  $\alpha$ -helical bundle, parallel (all up) and antiparallel (up–down). To analyze the orientation of the metal-complexed IZ-3adH, a fluorescent probe, acridine, was coupled to the N-terminus of the IZ-3adH. As shown in Figure 4, the acridinyl-modified IZ-3adH had the typical fluorescence spectrum of unassociated acridine in the absence of metal ions. Upon the addition of  $\text{Ni}(\text{II})$ , the fluorescence was quenched to below one-seventh of the original fluorescence intensity, suggesting that the metal-complexed peptide has the parallel orientation in the bundle structure.

Figure 5 shows the downfield region of the  $^1\text{H}$  NMR spectra of the IZ-3adH titrated with  $\text{NiCl}_2$ . In the absence of  $\text{Ni}(\text{II})$ , the aromatic protons from a Tyr residue appear at 6.87 and 7.20 ppm. These chemical shifts are typical for a flexible Tyr residue in a random coil structure. The  $\text{Ni}(\text{II})$  binding resulted in a high-field shift of the NMR resonances of the Tyr residue, suggesting that the Tyr residue in the peptide– $\text{Ni}(\text{II})$  complex was not completely flexible, but was constrained near the core of the  $\alpha$ -helical bundle.<sup>33</sup> Only a single set of Tyr protons was observed

(31) (a) Graddis, T. J.; Myszkka, D. G.; Chaiken, I. M. *Biochemistry* **1993**, *32*, 12664–12671. (b) Zhou, N. E.; Kay, C. M.; Hodges, R. S. *Protein Eng.* **1994**, *7*, 1365–1372. (c) Kohn, W. D.; Kay, C. M.; Hodges, R. S. *Protein Sci.* **1995**, *4*, 237–250.

(32) See the Supporting Information.

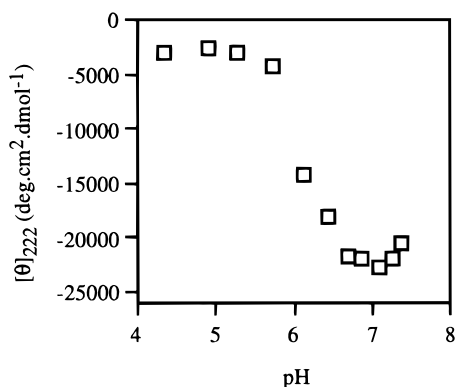


**Figure 7.** pH dependence of the IZ-3adH in the presence of NiCl<sub>2</sub>. Measurements were performed in 10 mM Tris-HCl, 100 mM NaCl, and 30  $\mu$ M NiCl<sub>2</sub> at various pH conditions. The peptide concentrations were 20  $\mu$ M.

after the addition of 1 equiv of Ni(II) to the three IZ-3adH molecules. Further addition of Ni(II) did not change the spectrum. These results strongly suggest that the three IZ-3adH molecules were complexed with a single Ni(II) ion.

Taken together with the results from the CD, sedimentation equilibrium, fluorescence quenching, and NMR studies, we conclude that the transition metals induce the self-assembly of the IZ-3adH peptide into a triple-stranded parallel  $\alpha$ -helical bundle and that there is only one metal ion within the peptide-metal complex.

The Ni(II) complex of the IZ-3adH was analyzed by thermal denaturation to assess the stability and the cooperativity of their association (Figure 6). Although the baseline was sloped in the low-temperature range (below 25  $^{\circ}$ C), the peptide-metal complex exhibited a reasonably cooperative unfolding curve,

with a midpoint of about 50  $^{\circ}$ C. The metal binding site divides the peptide into two regions, the N-terminal two heptads and the C-terminal heptad. The shorter C-terminal region has only two turns of the helix, which might cause the gradually unfolding at the low temperatures.

**Characterization of the Metal Binding Site.** Binding of the paramagnetic Ni(II) ion leads to perturbations in both the line width (relaxation) and the chemical shift of the NMR resonances of a peptide ligand.<sup>34</sup> Both effects are dependent on the distance from the nucleus to the metal ion ( $1/r^6$  and  $1/r^3$  dependence, respectively).<sup>34</sup> In the absence of Ni(II), the imidazole protons from the His residues appear at 7.03 and 7.90 ppm (Figure 5). These chemical shifts are typical for the  $\delta$ - and  $\epsilon$ -CH protons of His residues in a random coil structure. Upon the addition of the Ni(II), these peaks gradually broadened and finally disappeared, indicating that all of the His residues are magnetically equivalent and are near the Ni(II) ion. These results suggest that all six of the His residues might ligate the metal ion.

Since the imidazolyl group of a His residue has a  $pK_a$  value of about 6.0, the His residue does not act as a ligand under acidic conditions, due to protonation. To determine the effect of pH on the metal complex of the IZ-3adH, a pH titration curve was obtained by monitoring the  $[\theta]_{222}$  in the presence of Ni(II) (Figure 7). As the pH was decreased, the  $\alpha$ -helicity of the peptide decreased, with a transition midpoint of pH 6. This result also supports the proposal that the His residues are the ligands for the metal binding.

**Affinities of IZ-3adH for Metal Ions.** The binding of each metal ion to the IZ-3adH was indirectly evaluated by monitoring the fraction of folded peptide by CD spectroscopy. Titrations of the IZ-3adH with Co(II), Ni(II), Cu(II), or Zn(II) were performed at a peptide concentration of 20  $\mu$ M. As described

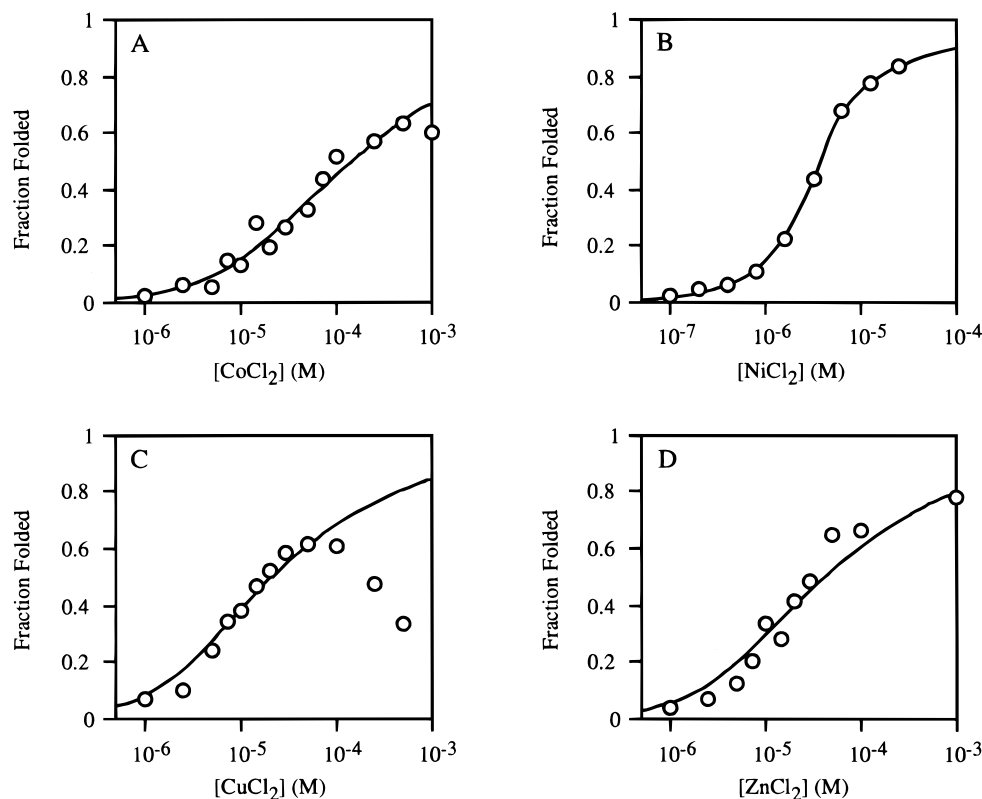


**Figure 8.** Metal ion titration profiles of the IZ-3adH, as monitored by CD. The fraction of folded peptide was plotted against the initial metal ion concentration. Measurements were performed in 10 mM Tris-HCl and 100 mM NaCl (pH 7.3) at 20  $^{\circ}$ C. The peptide concentrations were 20  $\mu$ M. The  $[\theta]_{222}$  of the metal-saturated forms of the peptide,  $[\theta]_{\infty}$ , are (A) CoCl<sub>2</sub>, -25 500; (B) NiCl<sub>2</sub>, -27 400; (C) CuCl<sub>2</sub>, -22 200; (D) ZnCl<sub>2</sub>, -29 200 deg cm<sup>2</sup> dmol<sup>-1</sup>. The data were fitted using a nonlinear least-squares fitting procedure, as described in the Experimental Section.

above, the results from the sedimentation equilibrium analyses and the Ni(II) titration study by NMR revealed that three IZ-3adH molecules bound one metal ion in the complex. Therefore, the data were fitted using a nonlinear least-squares fitting procedure, assuming a two-state model,  $1/3M + P \leftrightarrow 1/3(P_3M)$ . As shown in Figure 8, all of the metal ions, except Cu(II), increased the fraction of folded peptide with increases in their concentrations. Ni(II) had the highest affinity, with a  $K_d$  of  $5.0 \pm 0.3 \mu\text{M}$ . Both Co(II) and Zn(II) bind to the IZ-3adH less tightly than Ni(II), with a  $K_d$  of  $35 \pm 1 \mu\text{M}$  for Co(II) and  $23 \pm 2 \mu\text{M}$  for Zn(II). The result for Cu(II) is somewhat different from those for the others. Cu(II) induced the  $\alpha$ -helical formation of the peptide at a concentration below  $100 \mu\text{M}$ . However, excess Cu(II) destabilized the folding. Fitting of the data from 1 to  $100 \mu\text{M}$  yields a  $K_d$  of  $17 \pm 1 \mu\text{M}$  for Cu(II).

The NMR-detected hydrogen exchange study provides valuable information for protein folding.<sup>28</sup> In the case of the IZ-3adH–Ni(II) complex, the most protected amide protons were detectable even after 4–5 h (Figure 9). Their observed exchange rate constant ( $k_{\text{ex}}$ ) was about  $1.6 \times 10^{-4} \text{ s}^{-1}$ , which corresponds to an unfolding equilibrium constant ( $K_{\text{op}}$ ) of  $5 \times 10^{-6}$  and to an unfolding free energy ( $\Delta G_{\text{op}}$ ) of 7.2 kcal/mol, for a single IZ-3adH in the peptide–metal complex. This  $\Delta G_{\text{op}}$  value is in good agreement with a dissociation free energy ( $\Delta G_{\text{diss}}$ ) of about 7.1 kcal/mol, which is calculated from the  $K_d$  determined by Ni(II) titration using CD, suggesting that the most protected amide protons of the Ni(II)-complexed peptide exchange via global unfolding. These results provide evidence that the IZ-3adH–Ni(II) complex has natively like structural uniqueness and that the uncomplexed IZ-3adH was fully unfolded.

## Discussion

Designed coiled coil peptides with the capacity of metal ion induced self-assembly are useful tools to control the associations of functional domains attached to the peptides. In this study, we have constructed a metallopeptide (IZ-3adH), in which two His residues are substituted for two Ile residues of the parallel triple-stranded coiled coil peptide (IZ). Structural characterization of the metallopeptide showed that transition metal ions, in particular Ni(II), induced self-assembly of the peptide into a parallel triple-stranded  $\alpha$ -helical bundle. Although there was no evidence of the formation of a coiled coil, even the  $\alpha$ -helical bundle is sufficient to control the associations of the attached domains.

It was recently reported that a coiled coil peptide, L16C, formed the Hg(II) binding site in the hydrophobic interior and that the oligomerization state of the L16C–Hg(II) complex changed from a trimer at high peptide/metal ratios to a dimer at low peptide/metal ratios.<sup>35</sup> We observed only the three IZ-3adH:one Ni(II) complex at high peptide/metal ratios in the Ni(II) titration study by NMR. In the sedimentation equilibrium analysis, the IZ-3adH complexes with Ni(II), Co(II), and Zn(II) were trimeric, even at a low peptide/metal ratio. These results suggest that the oligomerization state of these complexes is independent of the peptide/metal ratio.

The oligomerization state of the IZ-3adH–Cu(II) complex could not be determined by sedimentation equilibrium analysis.

(33) This finding is supported by the result that the NOEs between the aromatic protons and the methyl group at 0.81 ppm (probably the Ile residue at position 4) were observed (data not shown).

(34) Jardetzky, O.; Roberts, G. C. K. *NMR in Molecular Biology*; Academic Press Inc.: Orlando, FL, 1981; pp 69–114.

(35) Dieckmann, G. R.; McRorie, D. K.; Tierney, D. L.; Utschig, L. M.; Singer, C. P.; O'Halloran, T. V.; Penner-Hahn, J. E.; DeGrado, W. F.; Pecoraro, V. L. *J. Am. Chem. Soc.* **1997**, *119*, 6195–6196.

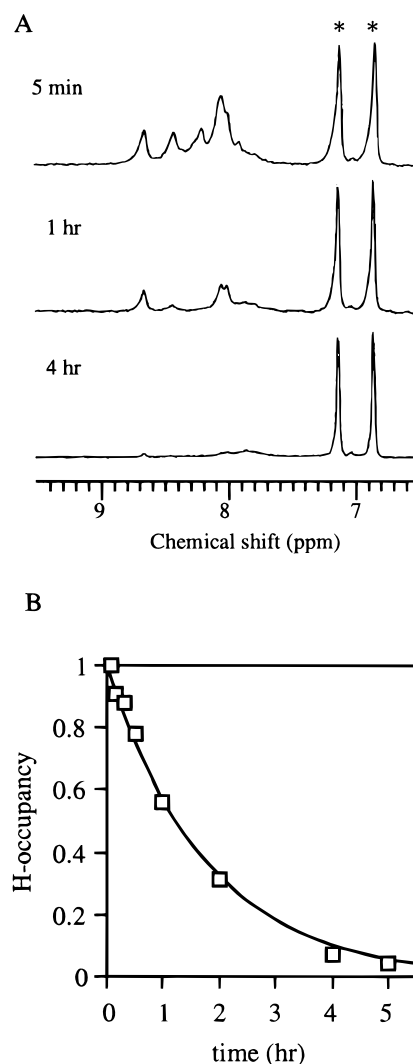


**Figure 9.** (A)  $^1\text{H}$  NMR amide hydrogen exchange studies of the IZ-3adH in the presence of  $\text{NiCl}_2$ . The measurements were performed in  $^2\text{H}_2\text{O}$  at  $25^\circ\text{C}$ . The peptide and  $\text{NiCl}_2$  concentrations were 1.0 and 0.4 mM, respectively. The resonances indicated by asterisks arise from a Tyr residue. (B) Time course of  $^1\text{H}$  occupancy of the slowest exchanging amide proton of the IZ-3adH in the presence of  $\text{NiCl}_2$ . The data were fitted for the exponential decay to yield a  $k_{\text{ex}}$  of about  $1.6 \times 10^{-4} \text{ s}^{-1}$ , leading to an unfolding equilibrium,  $K_{\text{op}}$ , of about  $5 \times 10^{-6}$ .

The Ile-zipper coiled coil preferentially forms a triple strand.<sup>2c,8f</sup> On the other hand, Cu(II) prefers four-coordinate geometry,<sup>36</sup> which might be formed in the postulated double-stranded IZ-3adH. Therefore, we hypothesize that the Cu(II)-complexed IZ-3adH forms the trimer at high IZ-3adH/Cu(II) ratios and the dimer at low peptide/metal ratios. This hypothesis can explain the strange folding behavior of IZ-3adH in the Cu(II) titration (Figure 8C). At high peptide/metal ratios, the intrinsic conformational preference of the peptide results in the trimer forming a complex with Cu(II). Under conditions with an excess of metal, however, the favorable four-coordinate geometry of the Cu(II) binding site forces a change of the oligomerization state to the dimer, in which the unfavorable side-chain packings of the Ile residues destabilize the  $\alpha$ -helical structure.<sup>2c</sup>

On the basis of the above discussion, we fit the titration data of IZ-3adH with metal ions to a two-state binding model,  $1/3M + P \leftrightarrow 1/3(P_3M)$ . In the case of the Cu(II), we used the data below  $100 \mu\text{M}$  Cu(II) concentration. The data fit well to the

(36) Sundberg, R. J.; Martin, R. B. *Chem. Rev.* **1974**, *74*, 471–517.

model and gave a  $K_d$  of  $35 \pm 1 \mu\text{M}$  for Co(II),  $5.0 \pm 0.3 \mu\text{M}$  for Ni(II),  $17 \pm 1 \mu\text{M}$  for Cu(II), and  $23 \pm 2 \mu\text{M}$  for Zn(II). However, the actual mechanism of the metal binding may be expressed as a multistate binding,  $1/3[\text{M} + 3\text{P}] \leftrightarrow 1/3[\text{PM} + 2\text{P}] \leftrightarrow 1/3[\text{P}_2\text{M} + \text{P}] \leftrightarrow 1/3(\text{P}_3\text{M})$ . In the Ni(II) titration study by NMR, only two sets of Tyr signals, from the uncomplexed structure and the final complexed one, were observed throughout the titration. Signals from intermediates were not observed. These results suggest that the metal binding in the multistate mechanism induces highly positive cooperativity, in which the first peptide binding to the metal enhances the second and third peptide binding.

Elucidation of the coordination geometry of the metal binding site is a significant subject. We incorporated six His residues into the hydrophobic core of the triple-stranded coiled coil. The results obtained from both the Ni(II) titration by NMR and the pH titration by CD suggest that all six of the His residues ligate the metal ion. The metal ion selectivity also provides additional information for the coordination geometry. The affinities of a single imidazole for the transition metal ions have been well characterized and follow the order  $\text{Cu(II)} > \text{Ni(II)} > \text{Zn(II)} \approx \text{Co(II)}$ .<sup>36</sup> All of these metal ions can bind six imidazoles, except for Cu(II), which binds only four imidazoles, even in the presence of excess imidazole.<sup>36</sup> Therefore, Ni(II) is considered to be the most favorable metal ion to form a six-imidazole coordinate complex with octahedral geometry.<sup>36</sup> We found that the affinities of the IZ-3adH for metal ions followed the order  $\text{Ni(II)} > \text{Cu(II)} > \text{Zn(II)} \approx \text{Co(II)}$ . The highest affinity for Ni(II) suggests that the binding site of the triple-stranded IZ-3adH has six-coordinate octahedral geometry. Taken together, we conclude that the six His residues in the metallopeptide coordinate to a single metal ion with an octahedral geometry.

Many metal binding sites with various geometries have been incorporated into proteins and peptides.<sup>14</sup> Although some of these metal binding sites coordinate a metal ion with six-coordinate octahedral geometry, they were constructed using either bipyridine or porphyrin as ligands.<sup>37,38</sup> To our knowledge, IZ-3adH is the first designed metallopeptide in which a metal

binding site with octahedral geometry is formed by six His residues. Such His-rich metal binding sites in the hydrophobic environment are observed in natural metalloenzymes.<sup>39</sup> In addition, the IZ-3adH–metal complex has natively like structural uniqueness, as determined by the cooperative thermal unfolding and the hydrogen exchange through global unfolding. Therefore, the IZ-3adH peptide could be a potential scaffold for the further design of synthetic metalloenzymes.

In this paper, we incorporated a novel metal binding site in a coiled coil peptide. The metallopeptide, IZ-3adH, underwent metal ion induced self-assembly into a parallel triple-stranded  $\alpha$ -helical bundle. The metal-complexed IZ-3adH also exhibited a pH-dependent conformational change. Thus, the IZ-3adH peptide can mediate the associations of attached functional domains, in response to a transition metal ion and pH. In contrast to the previously designed, double-stranded  $\text{Gla}_2\text{Nx}$ ,<sup>16</sup> the IZ-3adH peptide is applicable as a homotrimerization template. In addition, the six-His system described here could be applied to a designed heterotrimeric helical bundle. It would enable one to control the heterotrimerization of three different functional domains. Furthermore, the IZ-3adH peptide consists of only codon-encoded amino acids, and therefore, it is applicable to both in vitro and in vivo purpose. Thus, the IZ-3adH peptide provides a powerful tool to incorporate interesting functions into de novo designed proteins and peptides.

**Supporting Information Available:** Data of the sedimentation equilibrium analysis of the IZ-3adH in the presence of  $\text{NiCl}_2$  (1 page, print/PDF). See any current masthead page for ordering information and Web access instructions.

JA982768D

(37) (a) Lieberman, M.; Sasaki, T. *J. Am. Chem. Soc.* **1991**, *113*, 1470–1471. (b) Ghadiri, M. R.; Soares, C.; Choi, C. *J. Am. Chem. Soc.* **1992**, *114*, 825–831.

(38) (a) Choma, C. T.; Lear, J. D.; Nelson, M. J.; Dutton, P. L.; Robertson, D. E.; DeGrado, W. F. *J. Am. Chem. Soc.* **1994**, *116*, 856–865. (b) Robertson, D. E.; Farid, R. S.; Moser, C. C.; Urbauer, J. L.; Mulholland, S. E.; Pidikiti, R.; Lear, J. D.; Wand, A. J.; DeGrado, W. F.; Dutton, P. L. *Nature* **1994**, *368*, 425–432.

(39) Klemba, M.; Regan, L. *Biochemistry* **1995**, *34*, 10094–10100.